JOURNAL OF CATALYSIS 120, 29–45 (1989)

Active Sites of Molybdenum Sulfide Catalysts Supported on Al_2O_3 and TiO_2 for Hydrodesulfurization and Hydrogenation

YASUAKI OKAMOTO, AKINORI MAEZAWA,[1] AND TOSHINOBU IMANAKA

Department of Chemical Engineering, Faculty of Engineering Science, Osaka University, Toyonaka, Osaka 560, Japan

Received February 22, 1989; revised June 6, 1989

A comparative characterization of sulfided MoO_3/Al_2O_3 and MoO_3/TiO_2 catalysts was conducted by using LRS, XPS, IR, and TDS of NO. On the basis of the characterization, the active sites were estimated for the hydrodesulfurization of thiophene and hydrogenation of butadiene. The LRS and XPS results indicated that sulfided MoO_3/Al_2O_3 catalysts consisted of MoS_2-like phases and Mo(V) species, while sulfided MoO_3/TiO_2 catalysts was fully sulfided to MoS_2-like phases. The TDS of NO demonstrated that there were at least two distinctly different NO adsorption sites on sulfided molybdenum catalysts. They were assigned to triply (α) and doubly (β) cus Mo-sites on the basis of the H_2S–NO coadsorption. The fractions of α- and β-sites depended on both molybdenum loading and support, suggesting a variation in the morphology of MoS_2-like phases. The number of α-sites was linearly correlated to the activity for the hydrogenation of butadiene at 273 K, being independent of the support. This suggests that α-sites are responsible for the hydrogenation. Hydrogenation cycles involving α-sites are proposed at low and high reaction temperatures and in the presence and absence of H_2S. With the HDS reaction, separate parabolic correlations were obtained for the MoO_3/Al_2O_3 and MoO_3/TiO_2 catalysts between the activity and NO adsorption, suggesting dual sites as the HDS active centers and negative effects of molybdenum sulfide–support interactions.

INTRODUCTION

Molybdenum sulfide hydrodesulfurization (HDS) catalysts have been extensively investigated because of their academic interest as well as their industrial importance (*1, 2*). To obtain information on the active sites of the catalysts, correlations between the HDS activities of promoted or unpromoted molybdenum sulfide catalysts and the amount of adsorbed probe molecules have been examined by many workers. Tauster *et al.* (*3*) showed a linear correlation between the HDS activity of dibenzothiophene and O_2 adsorption for unsupported MoS_2 catalysts. As for HDS over sulfided MoO_3/Al_2O_3 catalysts, linear correlations were also obtained for O_2 adsorption by Bachelier *et al.* (*4*) and Jung *et al.* (*5*), while parabolic relations were reported by Zwierczak *et al.* (*6*) and Topsøe *et al.* (*7*). The amount of NO adsorption was fairly well correlated to the thiophene HDS activity of MoO_3/Al_2O_3 catalysts (*5, 7–10*), while no good linear correlations was obtained for the hydrogenation of 1-hexene (673 K) (*9*), suggesting different active sites for the HDS and hydrogenation. However, the configuration of the active sites on sulfided molybdenum catalysts is not yet sufficiently unveiled for HDS and hydrogenation.

In the present study, a NO desorption technique was applied to molybdenum sulfide catalysts supported on TiO_2 and Al_2O_3 in order to reveal the active sites for the HDS of thiophene and the hydrogenation of butadiene and to obtain some insights into support effects on the catalytic behaviors of sulfided molybdenum catalysts.

With respect to the effect of support on the HDS activity of molybdenum sulfides, Ng and Gulari (*11*) have reported that TiO_2-

[1] Present address: Shizuoka University, Hamamatsu, Japan.

0021-9517/89 $3.00

supported molybdenum sulfide catalysts are more active in thiophene HDS reactions than Al_2O_3-supported catalysts. Nishijima and co-workers (*12, 13*) have shown similar results for the hydrocracking of diphenylmethane (10 wt% MoO_3). According to MuraliDhar *et al.* (*14*), however, a MoO_3/Al_2O_3 catalyst showed higher HDS performance than a MoO_3/TiO_2 catalyst (8 wt% Mo). In contrast to HDS, the hydrogenation activity of Al_2O_3-supported catalysts has been reported to be higher than that of TiO_2-supported catalysts (*12–14*). It is apparent that the catalytic behavior of molybdenum sulfide depends strongly on the support.

Several workers (*15–18*) have characterized molybdenum species supported on TiO_2 in an oxidic state by using X-ray photoelectron and laser Raman spectroscopies and a temperature programmed reduction technique. Their results are in good agreement with each other. At a low loading level of MoO_3 (i.e., under a monolayer coverage) surface molybdate species interacting with the support are formed, whereas at a higher MoO_3 content crystalline MoO_3 is detected. These results are analogous to those for Al_2O_3-supported catalysts (*1, 19, 20*). Sulfided MoO_3/Al_2O_3 catalysts have been characterized in detail by many workers (*1, 2*) using XPS (*21, 22*), LRS (*23, 24*), EXAFS (*25*), and other techniques (*24, 26*). Nevertheless, detailed characterization of sulfided MoO_3/TiO_2 catalysts has rarely been carried out.

In order to address the configuration of the active sites on molybdenum sulfides supported on Al_2O_3 and TiO_2, NO adsorption studies were carried out by using IR and thermal desorption spectroscopies (TDS). X-ray photoelectron (XPS) and laser Raman (LRS) spectroscopies were also employed to characterize the sulfided catalysts.

EXPERIMENTAL

γ-Al_2O_3 was supplied by the Catalysis Society of Japan as a reference catalyst (JRC-ALO-4, BET surface area 163 $m^2\ g^{-1}$) (*20*). TiO_2 was provided by Nippon Aerosil Co. (Degussa, P-25, 53 $m^2\ g^{-1}$). Supported molybdenum catalysts were prepared by an incipient impregnation method. The molybdenum concentration per surface area was adjusted to be 6.4–118 $\times$ 10^{13} Mo cm^{-2} (1–23 wt% MoO_3). An aqueous solution of appropriate concentration of ammonium heptamolybdate (Nakarai Chemicals) was added to the support and kneaded for 10 min at room temperature. Subsequently, the catalyst slurry was dried at 383 K for 18 h, followed by 5-h calcination in air at 823 K for Al_2O_3 or at 773 K for TiO_2. The lower calcination temperature for the MoO_3/TiO_2 catalysts was adopted to avoid the sintering of TiO_2.

Presulfidation of the catalyst was carried out at 673 K for 1.5 h in a stream of an atmospheric pressure of H_2S/H_2 (0.1, 500 ml STP min^{-1}). Subsequently, the HDS reaction of thiophene was carried out at the same temperature in a stream of an atmospheric pressure of thiophene/H_2 (1.6% thiophene, 1 liter STP min^{-1}), followed by the measurement of an averaged catalytic activity at the reaction time 1–1.5 h. The reaction gas was analyzed by glc.

After the HDS reaction, the catalyst was treated with a stream of an atmospheric pressure of deoxygenated and dehydrated H_2 at 673 K for 1 h and then evacuated for 1 h at the same temperature. After the catalyst was cooled to room temperature under a dynamic vacuum, the amount of NO chemisorption was volumetrically measured at room temperature (the catalyst was exposed to NO for 30 min and evacuated for 1 h, accompanied by NO physisorption experiments).

The hydrogenation of 1,3-butadiene was carried out at 273 K over a molybdenum catalyst using a closed circulation system (220 ml). The pressure of butadiene/H_2 (1/2) was 7.3 kPa. The catalysts had been presulfided under the same conditions as for the HDS reaction, followed by an H_2-treatment at 673 K for 1 h. The sample was then evac-

uated at 673 K for 1 h prior to the hydrogenation reaction.

The XP spectra of sulfided catalysts were recorded without exposing to air. The XPS measurements were made on a Hitachi 507 photoelectron spectrometer using Al$K\alpha_{1,2}$ radiation (1486.6 eV). The anode was operated at 9 kV and 50 mA. Assuming linear backgrounds, XPS intensity ratios were determined by using the integrated areas of the Mo3*d*, Al2*p*, and Ti2*p* levels. Binding energies (BE) were referenced to the support level, which had been determined by using the C1*s* level at 285.0 eV due to adventitious carbon.

The measurement of IR spectra and TDS of NO and LRS were made *in situ* for sulfided catalyst samples. The sample was exposed to NO at room temperature for IR or TDS study. The IR spectra of the catalyst were recorded in a transmittance mode at room temperature by using self-supporting wafers on a Hitachi EPI-G double beam spectrophotometer.

The TDS study of NO adsorbed on a sulfided catalyst was conducted in a dynamic vacuum by increasing the desorption temperature at a rate of 1.8 K min^{-1} from room temperature to ca. 570 K. Evolved gases were continuously and repeatedly analyzed by a mass filter (ULVAC, MSQ-105A).

The *in situ* LR spectra were obtained at room temperature with a JASCO R-800 spectrometer equipped with a double monochromator. The 514.5-nm line of a NEC GLS-3200 Ar^+ laser was used for excitation at an intensity of 150 mW at the source. A spectral resolution was 5 cm^{-1}. The spectra of sulfided catalysts were obtained without exposure to air or moisture by vacuum sealing in Pyrex glass tubes.

RESULTS

The HDS of thiophene was carried out at 673 K over a molybdenum catalyst presulfided with H_2S/H_2 (1/10) at 673 K. The sulfided catalyst was characterized by LRS and XPS. Figure 1 shows the LR spectra of presulfided Al_2O_3- and TiO_2-supported catalysts. The Mo=O stretching vibration bands around 960 cm^{-1} in the oxidic catalysts, which are attributed to interaction species (*18–20, 27, 28*), were completely eliminated on presulfidation. The spectra (a, b, and e) show two bands characteristic of MoS_2 (380 and 405 cm^{-1}) (*23, 29*), the lower wavenumber band for the 2.4-wt% MoO_3/Al_2O_3 catalyst (a) being indistinct due to its weak and broad nature compared to the 405-cm^{-1} band. With the 4.8-wt% MoO_3/TiO_2 catalyst (d), the relevant spectral region was obscured by a relatively intense band at 398 cm^{-1} assigned to TiO_2 (anatase) (*18*). However, a weak band around 405 cm^{-1} suggests the presence of the doublet bands due to MoS_2. The LR signals around 400 cm^{-1} were completely disturbed for the MoO_3/TiO_2 catalysts con-

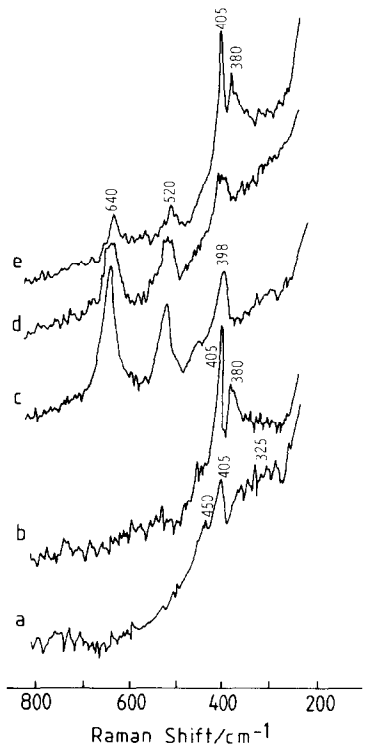

FIG. 1. *In situ* laser Raman spectra for sulfided molybdenum catalysts: (a) MoO_3/Al_2O_3 (2.4); (b) MoO_3/Al_2O_3 (13.0); (c) MoO_3/TiO_2 (2.9); (d) MoO_3/TiO_2 (4.8); and (e) MoO_3/TiO_2 (9.1). The number in parentheses represents MoO_3 content (wt%).

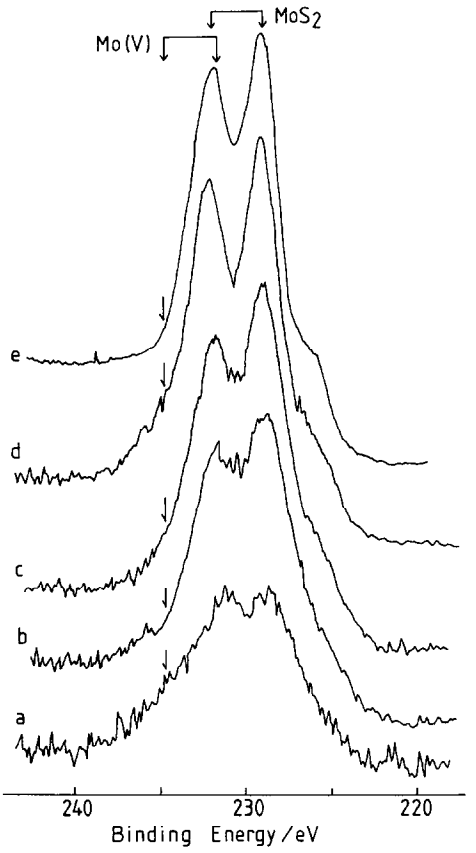

FIG. 2. Mo3*d* XP spectra of sulfided MoO_3/Al_2O_3 catalysts after the thiophene HDS and subsequent H_2-treatment at 673 K. The molybdenum contents are (a) 2.4, (b) 9.1, (c) 13.0, and (d) 23.1 wt% MoO_3. The spectrum (e) shows the Mo3*d* band for MoS_2.

taining less than 2.9 wt% and then no decisive conclusions were obtained from LRS. The peaks at 640 and 520 cm^{-1} for the MoO_3/TiO_2 are also attributed to TiO_2 (anatase) (*18*).

In addition to these peaks, broad structures were observed around 325 and 450 cm^{-1} for the 2.4-wt% MoO_3/Al_2O_3 (a). With the other catalysts, no evidence was obtained to the presence of these bands, taking into consideration a weak band at 468 cm^{-1} due to MoS_2 (*23*). It was shown previously (*24*) that the LR bands around 325 and 450 cm^{-1} were the main signals when H_2-prereduced 13-wt% MoO_3/Al_2O_3 was sulfided during the HDS of thiophene at 673 K and that these bands were replaced by sharp bands at 380 and 405 cm^{-1} after a prolonged reaction time (12 h). These broad bands were assigned to oxysulfide or highly dispersed amorphous molybdenum sulfides (*24*).

The Mo3*d* XP spectra for the sulfided MoO_3/Al_2O_3 and MoO_3/TiO_2 catalysts are shown in Figs. 2 and 3, respectively. Before the XPS measurements, the catalyst was used for the HDS reaction of thiophene and subsequently treated with an atmospheric pressure of H_2 at 673 K. The H_2-treatment was conducted with an intention to eliminate possible carbon deposits and labile sulfur atoms which are expected to be in a dynamic equilibrium with the reaction gas during the HDS at 673 K. The XP spectral features in Figs. 2 and 3 were not essentially varied by the H_2-treatment.

The BE values of the Mo3$d_{5/2}$ band for the sulfided catalysts are summarized in Table 1. These values are close to that of

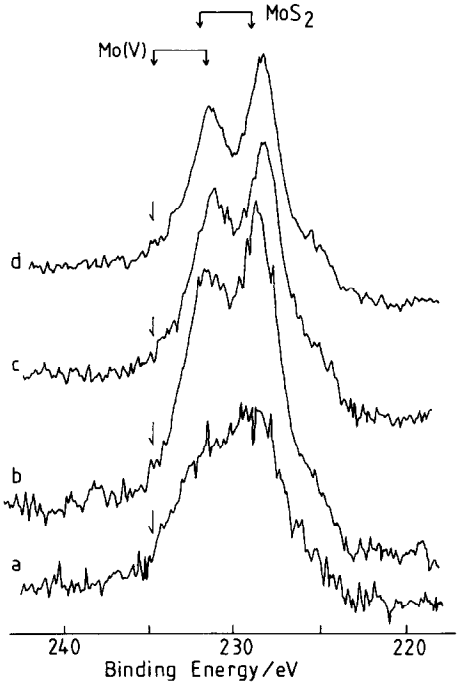

FIG. 3. Mo3*d* XP spectra of sulfided MoO_3/TiO_2 catalysts after the thiophene HDS reaction and subsequent H_2-treatment at 673 K. The molybdenum contents are (a) 1.0, (b) 2.9, (c) 4.8, and (d) 9.1 wt% MoO_3.

TABLE 1

XPS Results on the Supported Molybdenum Sulfide Catalysts[a]

Molybdenum content (wt%)	Molybdenum content (10^{13} Mo cm^{-2})	BE of Mo3$d_{5/2}$ (eV)	S/Mo atomic ratio
	Al_2O_3 (Al2p = 74.0 eV)		
2.4	6.4	228.9	1.40
4.8	12.8	228.8	1.45, 1.51[b]
9.1	25.6	228.9	1.75, 1.77[b]
13.0	38.3	228.9	1.70, 1.65[b]
16.7	51.1	229.1	1.65, 1.82[b]
23.1	76.7	229.0	1.79, 1.76[b]
	TiO_2 (Ti2$p_{3/2}$ = 458.5 eV)		
1.0	7.9	228.7	1.40, 2.2 ± 0.1[b]
2.9	23.6	228.7	1.36, 2.30[b]
4.8	39.3	228.3	1.59, 1.99[b]
9.1	78.6	228.4	1.86, 1.97[b]
13.0	118	228.3	1.80

[a] Measured after the HDS of thiophene and subsequent H_2-treatment at 673 K.

[b] Measured after presulfidation and subsequent evacuation at 673 K.

MoS_2 (229.0 eV) except for the MoO_3/TiO_2 containing ≧4.8 wt%. These reduced values are considered to result from differential charging of the catalyst surface as a consequence of insufficient electrical contact between molybdenum sulfides and support surface (*19, 30*).

With the MoO_3/Al_2O_3 and MoO_3/TiO_2 catalysts, the $I_{Mo}/I_{Al(Ti)}$ XPS intensity ratio linearly increased up to ca. 40 × 10^{13} Mo cm^{-2} (13 wt% MoO_3 for Al_2O_3 and 6 wt% for TiO_2) and deviated from the linear line at higher molybdenum concentration. It was found that the intensity ratio did not appreciably vary on presulfidation and HDS reaction. Accordingly, the XPS ratio suggests that molybdenum sulfides are uniformly dispersed on both catalyst systems below ca. 40 × 10^{13} Mo cm^{-2}.

As for the MoO_3/Al_2O_3 catalysts, the Mo3d band was broad and ill-resolved for the catalyst containing 2.4 wt% MoO_3, as shown in Fig. 2a. A shoulder peak at 226 eV on the Mo3d envelope is the S2s line (*21, 22*). The resolution of Mo3$d_{5/2}$ and 3$d_{3/2}$ sublevels increased with increasing molybdenum content. These XPS observations were previously noted (*22*). The BE values due to Mo(V) species (231.6 and 234.6 eV for Mo3$d_{5/2}$ and 3$d_{3/2}$, respectively) (*21*) are shown in Figs. 2 and 3. It is noteworthy that in Fig. 2 a weak hump, which cannot be seen for the spectrum of MoS_2 (e), is apparently observed around 234.6 eV in the spectra. This is indicative of the formation of Mo(V) species. The broad spectrum for the 2.4-wt% catalyst (a) is attributed to the presence of a considerable proportion of Mo(V) species. On the basis of the deconvolution of the Mo3d XP spectra, Li and Hercules (*21*) have quantitatively shown the presence of reduction- and sulfidation-resistant Mo(V) species on sulfided MoO_3/Al_2O_3 catalysts.

Contrary to the Al_2O_3-supported catalysts, the MoO_3/TiO_2 catalysts showed no significant XPS signal around 234.6 eV (Fig. 3) irrespective of the molybdenum loading. An ill-resolved spectrum for 1.0-wt% catalyst is considered to be due mainly to charging effects (*19, 22*) rather than the presence of Mo(V) species. The XP spectra in Figs. 2 and 3 apparently suggest that molybdenum species supported on TiO_2 are more readily reduced and sulfided than those on Al_2O_3.

It was found from the temperature-programmed reduction (TPR) experiments (5% H_2 in Ar, 5 K min^{-1}) that the reduction temperature and averaged oxidation number of reduced molybdenum on the TiO_2-supported catalyst were lower than those on the Al_2O_3-supported catalyst (oxidation number: ca. 4 for 4.8-wt% MoO_3/TiO_2 at 643 K and ca. 5 for 13-wt% MoO_3/Al_2O_3 at 693 K) at a similar surface molybdenum loading ca. 40 × 10^{13} Mo cm^{-2}.

The degree of sulfidation of molybdenum, S/Mo atomic ratio, was estimated from the S2p/Mo3d XPS intensity ratio by using MoS_2 as a standard compound. These values are also summarized in Table 1. A slight sulfur deposition on the TiO_2 surface

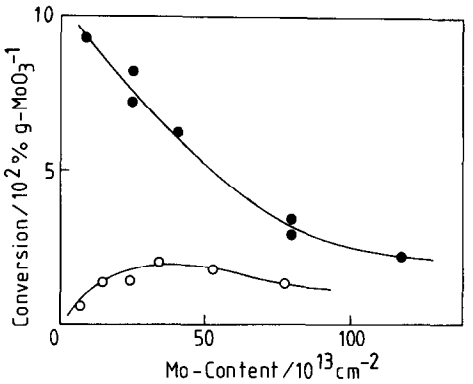

FIG. 4. Dependence of thiophene HDS activity of sulfided molybdenum catalyst at 673 K on the molybdenum content per surface area of the support: ○, MoO_3/Al_2O_3; ●, MoO_3/TiO_2.

was corrected (S2*p*/Ti2*p* = 0.011 and 0.014 after and before the H_2-treatment, respectively, and S2*p* = 163.9 eV) in the calculation of the S/Mo ratio for sulfided MoO_3/TiO_2. The sulfidation of Al_2O_3 was below the detection limit of the present XP spectrometer. With the Al_2O_3- and TiO_2-supported molybdenum sulfide catalysts, the S/Mo ratio was 1.6–1.8 except for the low molybdenum content catalysts, which showed slightly lowered S/Mo ratios (ca. 1.4).

The S/Mo ratios were also obtained for the catalysts just after the presulfidation and evacuation at 673 K for 1 h (before the reaction and subsequent H_2-treatment) and are summarized in Table 1. As for the MoO_3/Al_2O_3 catalysts, these S/Mo ratios were identical with the ratios after the reaction and subsequent H_2-treatment within the accuracy of the XPS measurements (±0.05). Nevertheless, the extent of sulfidation for the MoO_3/TiO_2 catalyst was considerably reduced by the reaction and H_2-treatment following the presulfidation.

The specific activity of the catalyst (thiophene conversion per g MoO_3) is shown in Fig. 4 as a function of surface molybdenum concentration (molybdenum loading per surface area of the support) to facilitate a strict comparison between the chemical nature of the supports by eliminating surface area effects. The specific activity of MoO_3/TiO_2 decreased with increasing molybdenum content, while that of MoO_3/Al_2O_3 showed a broad maximum at ca. 35×10^{13} Mo cm^{-2} (13 wt% MoO_3). Evidently, MoO_3/TiO_2 exhibited much higher specific activity than MoO_3/Al_2O_3. The higher efficiency of TiO_2-supported catalysts for HDS is consistent with the results of other workers (*11–13*).

The activities of the catalysts are summarized in Table 2 for the HDS of thiophene (673 K) and the hydrogenation of butadiene (273 K). In contrast to the HDS, the MoO_3/Al_2O_3 catalyst showed a hydrogenation activity comparable to or higher than that of the MoO_3/TiO_2 catalyst at a similar MoO_3 loading. This is in agreement with the results in the literature (*12, 13*).

In order to obtain some information about the active sites on the sulfided molybdenum catalysts for the HDS and hydrogenation reactions, a volumetric measurement of NO chemisorption was carried out at room temperature for the Al_2O_3- and TiO_2-supported catalysts after the HDS reaction and a subsequent H_2-treatment. The amounts of NO adsorption are presented in Table 2.

The IR study of NO adsorption on sulfided catalysts showed characteristic doublet signals at 1793 and 1696 cm^{-1} for the MoO_3/TiO_2 (2.9 wt%) and at 1791–1794 and 1700 cm^{-1} for the MoO_3/Al_2O_3 catalysts (2.4–16.7 wt%). The NO molecules on H_2-reduced molybdenum oxides showed IR bands at 1820 and 1710 cm^{-1}. These results are in good agreement with the previous results (*31*) and those of other workers (*32*). No IR bands of NO adsorbed on the support was observed.

The NO/Mo atomic ratios for sulfided catalysts are illustrated in Fig. 5 as a function of the molybdenum content per surface area of the support. The NO/Mo ratio for MoO_3/TiO_2 decreased as the molybdenum content increased, while the ratio for MoO_3/Al_2O_3 attained a maximum at 4.8

TABLE 2

NO Adsorptions on Molybdenum Sulfide Catalysts Supported on Al_2O_3 and TiO_2

MoO_3 content (wt%)	Amount of NO ads (10^{-5} mol g cat^{-1})			$\alpha/(\alpha + \beta)$	NO/Mo ratio	Catalytic activity[a]	
	total	α	β			HDS	HG
				Al_2O_3			
2.4	4.3	2.8	1.5	0.66	0.26	31	4.2
4.8	11.5	7.9	3.6	0.69	0.35	134	17.3
9.1	18.4	14.4	4.0	0.78	0.29	276	36.5
13.0	19.8	15.6[b]	4.2[b]	0.79[b]	0.22	554	31.0
16.7	21.8	17.4	4.4	0.80	0.19	620	39.9
23.1	23.0	18.2	4.8	0.79	0.14	683	43.9
				TiO_2			
1.0	5.8	3.2	2.6	0.56	0.84	162	2.6
2.9	10.8	6.2	4.6	0.57	0.54	340	8.0
4.8	11.1	6.7[b]	4.4[b]	0.60[b]	0.33	599	12.5
9.1	8.0	5.3	2.7	0.66	0.13	460	12.0
13.0	7.7				0.085	669	

[a] 10^{-8} mol g cat^{-1} s^{-1}. Reaction temperature, HDS of thiophene, 673 K; HG (hydrogenation) of butadiene, 273 K.

[b] Estimated by interpolation.

wt% MoO_3. It is apparent that at a similar surface molybdenum concentration the NO/Mo ratio for the MoO_3/TiO_2 is larger than that for MoO_3/Al_2O_3, in particular, below the molybdenum content 40 × 10^{13} Mo cm^{-2}. On the other hand, when the NO/Mo ratios are compared at a similar wt% of MoO_3, the NO/Mo ratio for the MoO_3/Al_2O_3 is higher than that for the MoO_3/TiO_2 except for <3 wt%. This is a consequence of a large difference in the surface area of the support.

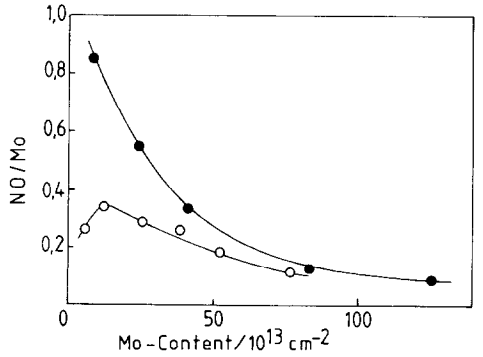

FIG. 5. Amount of NO adsorption over sulfided molybdenum catalyst as a function of the molybdenum content per surface area of the support: ○, MoO_3/Al_2O_3; ●, MoO_3/TiO_2.

It is interesting to examine whether the higher HDS activity of MoO_3/TiO_2 is ascribed to a larger concentration of catalytically active cus Mo-sites than that of MoO_3/Al_2O_3 (Fig. 4), as suggested from the results in Fig. 5. The turnover frequency (TOF) of the catalyst was calculated on the basis of the amount of NO adsorption, assuming that NO adsorbs on one Mo-site in a pair (*33–35*) and that NO adsorption sites constitute the catalytically active centers for the HDS of thiophene. The TOF values of MoO_3/Al_2O_3 and MoO_3/TiO_2 are depicted in Fig. 6 against the surface molybdenum concentration. The TOF values of both catalyst systems increased with increasing Mo-content and leveled off around 40 × 10^{13} Mo cm^{-2}. It is noteworthy that the TOF of the Al_2O_3-supported catalyst is about half of the TOF of the TiO_2-supported catalysts even at a high molybdenum content.

The TOF of the catalyst for the hydroge-

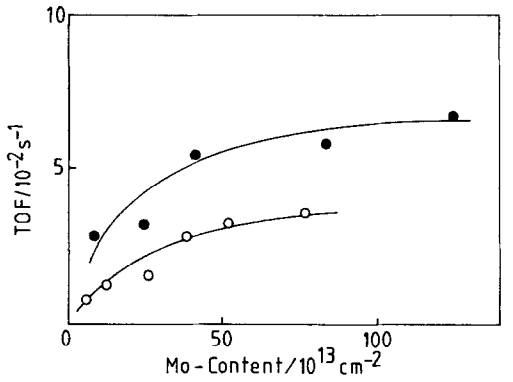

FIG. 6. TOF of the sulfided molybdenum catalyst for the HDS of thiophene at 673 K as a function of the molybdenum loading per surface area of the support: ○, MoO_3/Al_2O_3; ●, MoO_3/TiO_2.

nation of butadiene at 273 K was also calculated on the basis of the amount of NO adsorption. The preadsorption of NO was found to completely inhibit the hydrogenation over the MoO_3/Al_2O_3 and MoO_3/TiO_2 catalysts. The TOF is presented in Fig. 7 as a function of the surface molybdenum concentration. The TOF of both catalyst systems increased with increasing molybdenum content. It is evident in Fig. 7 that the TOF of the Al_2O_3-supported catalyst is higher than that of the TiO_2-supported catalyst, in contrast to the TOF for the HDS.

The results in Figs. 6 and 7 may suggest that there are several kinds of cus Mo-sites exhibiting different catalytic properties on supported molybdenum sulfide catalysts. TDS studies of NO adsorbed on the catalyst were conducted with an intention to differentiate these cus Mo-sites. The catalysts presulfided and subsequently H_2-treated at 673 K were exposed to NO at room temperature and evacuated for 30 min before the TDS experiments. Figure 8 shows the TDS profiles of NO (m/e = 30) for the sulfided MoO_3/Al_2O_3 and MoO_3/TiO_2 catalysts. Evidently, at least two distinctly different desorption peaks were observed at 395 ± 5 and 480 ± 5 K. The NO desorption peaks at lower and higher temperatures are denoted as α- and β-peaks here. The production of N_2O (m/e = 44) was observed during the TDS experiments. The intensity ratio of the signal of N_2O to that of NO was 0.95, almost independent of the desorption temperature and catalyst sample within the accuracy (±0.1) (On the other hand, the N_2O/NO signal intensity ratio was found to depend appreciably on the mass spectrometer used, probably because of different sensitivity factors). NO desorptions from the supports treated analogously to the catalyst were not detected under the present TDS conditions. Coupled with the IR results mentioned above, it is concluded that α- and β-NO desorb from sulfided cus Mo-sites.

A peak resolution of the TDS profile was graphically carried out assuming two symmetric desorption peaks with constant fwhm (full width at half maximum) values of 91 ± 3 K (α-peak) and 82 ± 3 K (β-peak). The separated component peaks are also illustrated in Fig. 8. The proportion of α-NO in the total NO adsorption ($\alpha/(\alpha + \beta)$) was calculated on the basis of the peak areas of α- and β-NO desorption. The respective amounts of α- and β-NO species were estimated from each proportion and the total amount of NO adsorption. They are summarized in Table 2. The $\alpha/(\alpha + \beta)$ ratios and then the amounts of respective NO species

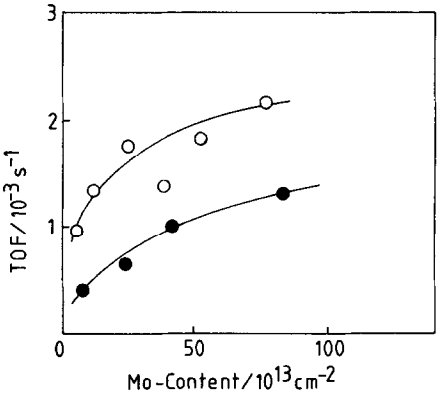

FIG. 7. TOF of the sulfided molybdenum catalyst for the hydrogenation of butadiene at 273 K as a function of molybdenum content per surface area of the support: ○, MoO_3/Al_2O_3; ●, MoO_3/TiO_2.

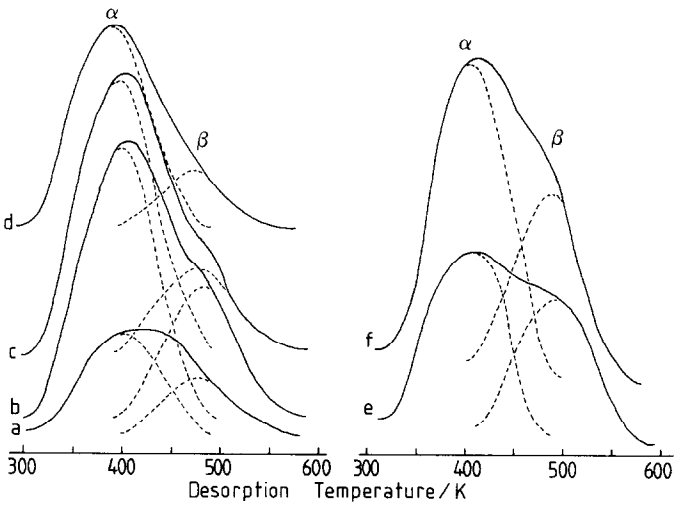

FIG. 8. TDS profiles (m/e = 30) of NO adsorbed on sulfided molybdenum catalysts: (a) MoO_3/Al_2O_3 (2.4); (b) MoO_3/Al_2O_3 (4.8); (c) MoO_3/Al_2O_3 (9.1); (d) MoO_3/Al_2O_3 (16.7); (e) MoO_3/TiO_2 (2.9); and (f) MoO_3/TiO_2 (9.1). The number in parentheses represents the MoO_3 content (wt%). The dashed curves show resolved α- and β-peaks.

were estimated for some catalysts by interpolation. It is evident from Fig. 8 and Table 2 that the proportion of α-NO increases with increasing molybdenum content for MoO_3/Al_2O_3 and MoO_3/TiO_2 and that the proportion of α-NO on MoO_3/Al_2O_3 is larger than that on MoO_3/TiO_2.

TDS experiments of coadsorption of NO and H_2S on sulfided MoO_3/Al_2O_3 catalysts were conducted to obtain some information about the adsorption sites of α- and β-NO. After the NO adsorption and subsequent evacuation at room temperature, the NO/catalyst system was exposed to H_2S (5.3 kPa) for 30 min and evacuated for 30 min at room temperature. The TDS spectra of NO are shown in Fig. 9 together with resolved desorption peaks. The N_2O/NO ratio was found to decrease by 50 ± 10%. The desorption temperatures of α- and β-peaks were about 425 and 480 K, respectively. The fwhm values were nearly equivalent to those in Fig. 8 except for the α-peak for the 16.7 wt% catalyst, which could not be deconvoluted without using a slightly increased fwhm (100 K). The $\alpha/(\alpha + \beta)$ ratios were 0.74 and 0.77 for the 9.1 and 16.7 wt% MoO_3/Al_2O_3 catalysts, respectively. They

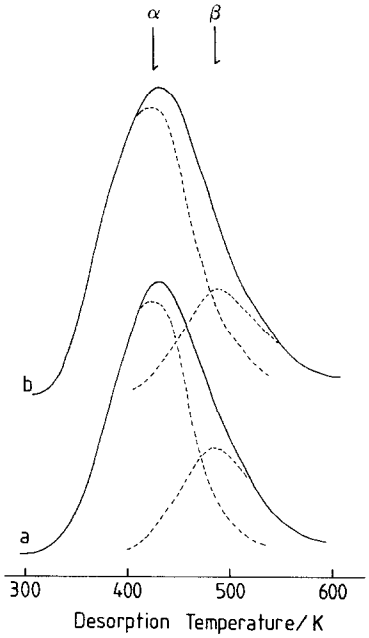

FIG. 9. TDS profiles (m/e = 30) of H_2S–NO coadsorption on sulfided MoO_3/Al_2O_3 catalysts. H_2S was introduced into the catalyst after preadsorption of NO. (a) 9.1 and (b) 16.7 wt% MoO_3. The dashed lines show resolved α- and β-peaks.

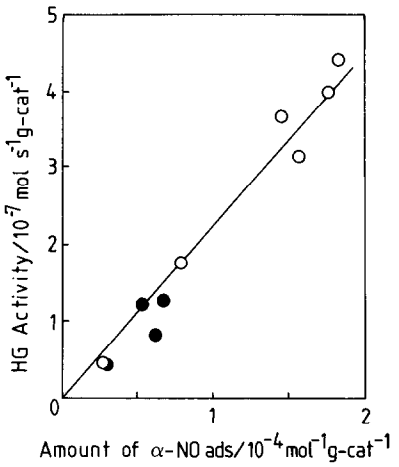

FIG. 10. Correlation between the activity of sulfided molybdenum catalyst and the amount of α-NO adsorption for the hydrogenation of butadiene at 273 K: ○, MoO_3/Al_2O_3; ●, MoO_3/TiO_2.

are close to the corresponding ratios for the adsorption of NO alone in Table 2. It is worth noting here that on the coadsorption of NO and H_2S the desorption temperature of α-NO is increased by 30 K, while that of β-NO is not affected within experimental accuracy (±5 K). The desorption peak of H_2S (m/e = 34) was observed at ca. 360 K. This is assigned to H_2S adsorbed on the bare Al_2O_3 surface (*36*). Hydrogen sulfide adsorbed on sulfided molybdenum sites is expected to desorb at >600 K (*36*).

In order to estimate the active sites for the hydrogenation of butadiene and the HDS of thiophene, correlations between the catalytic activities and the amount of NO adsorption were examined. The hydrogenation activity is shown in Fig. 10 as a function of the amount of α-NO species. A fairly good linear correlation was obtained that included both MoO_3/Al_2O_3 and MoO_3/TiO_2 (correlation coefficient r^2 = 0.97). The r^2 values for linear correlations between the hydrogenation activity and the total amount of NO adsorption and the amount of β-NO were 0.94 and 0.42, respectively. The best linear correlation was obtained for α-NO.

The HDS activity of the sulfided catalyst is plotted in Fig. 11 against the total amount of NO adsorption. In contrast to the hydrogenation, separate parabolic correlations were obtained for the Al_2O_3- and TiO_2-supported catalysts, the latter system exhibiting a higher HDS activity. Although other correlations were tried, the HDS activities of both catalyst systems were not linearly correlated to the amount of α- or β-NO adsorption. Also, they were not combined into a single curve.

DISCUSSION

A comparative characterization of sulfided MoO_3/Al_2O_3 and MoO_3/TiO_2 catalysts was carried out by using LRS and XPS. With the MoO_3/Al_2O_3 catalysts, the LR spectra in Fig. 1 are clearly indicative of the formation of MoS_2-like species (380 and 405 cm^{-1}). This is consistent with the LRS observations of Brown *et al.* (*29*) and Schrader and Cheng (*23*). In the case of oxidic MoO_3/Al_2O_3, it is generally established (*1, 19–22, 26*) that molybdate species are highly dispersed up to the so-called monolayer capacity of Al_2O_3 or 40–50 × 10^{13} Mo cm^{-2}. Since no appreciable change in the

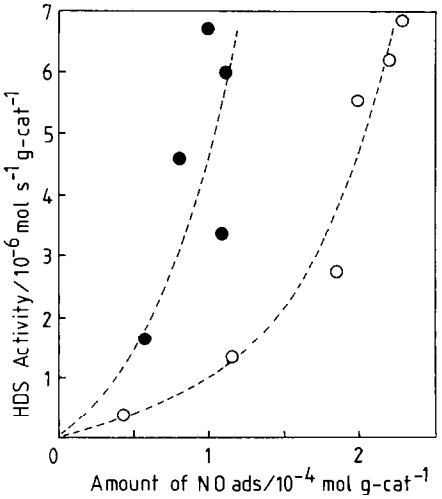

FIG. 11. Correlations between the activity of sulfided molybdenum catalyst and the total amount of NO adsorption for the HDS of thiophene at 673 K: ○, MoO_3/Al_2O_3; ●, MoO_3/TiO_2.

I_{Mo}/I_{Al} XPS intensity ratio was observed on sulfidation, it is suggested that the dispersion of molybdenum in the sulfided catalysts is as high as that in the oxidic precursor catalysts. The EXAFS results by Clausen *et al.* (*25*) have suggested that MoS_2-like species with crystallite size of about 1 nm are present on a sulfided MoO_3/Al_2O_3 catalyst (12.4 wt% MoO_3). On the basis of CO_2 adsorption, Zwierczak *et al.* (*26*) proposed the formation of monolayer slabs of MoS_2 for sulfided MoO_3/Al_2O_3 catalysts containing up to 11.5 wt% MoO_3. The present LRS and XPS results are in conformity with these propositions.

According to the XPS results by Hercules *et al.* (*19, 21*), the molybdenum species which are neither sulfided at 623 K nor H_2-reduced below Mo(V) even at 773 K are attributed to isolated molybdenum species in tetrahedral configurations (Mo_{tet}). The Mo3*d* XPS spectra in Fig. 2 for the sulfided MoO_3/Al_2O_3 catalysts clearly demonstrate the presence of Mo(V) species after the sulfidation at 673 K.

With the MoO_3/TiO_2 catalysts, the LR spectra in Fig. 1 show the formation of MoS_2-like species at above 4.8 wt% MoO_3 on sulfidation. Although no decisive conclusions could be obtained from the LR spectra, it is likely that MoS_2-like species are similarly formed below 2.9 wt% MoO_3. On the basis of the TPR results, the Mo–O–Ti bonds are considered to be more readily broken on reduction than the Mo–O–Al bonds (*20, 37*). In line with this, the XP spectra in Fig. 3 demonstrate that no residual Mo(V) species are present on the sulfided MoO_3/TiO_2 catalysts. It is concluded that molybdenum species supported on TiO_2 are fully sulfided, forming exclusively MoS_2-like species. This is in accord with the S/Mo ratios in Table 2 for the sulfided MoO_3/TiO_2 catalysts prior to the H_2-treatment. The S/Mo values (2.2–2.3) exceeding two suggest that the slab size of MoS_2 is considerably small and is the order of 1.5–2.2 nm for the MoO_3/TiO_2 catalysts containing less than 3 wt% MoO_3, on the basis of the triangle model proposed by Kasztelan *et al.* (*38*). The slab size of MoS_2 on MoO_3/TiO_2 is comparable to or slightly larger than that on MoO_3/Al_2O_3 (ca. 1 nm) (*25*) at a similar surface molybdenum content.

The S/Mo ratio for the presulfided MoO_3/Al_2O_3 catalyst was lower than that for the MoO_3/TiO_2 catalyst (Table 1). This apparently results from the presence of a considerable fraction of unsulfided Mo(V) species on the sulfided MoO_3/Al_2O_3 catalysts, as shown in Fig. 2. Assuming the content of Mo(V) species to be 9×10^{13} Mo cm^{-2} (isolated Mo_{tet}) in the 13 and 16.7 wt% MoO_3 catalysts (*20, 21*), the S/Mo ratios were calculated to be 2.2 and 1.9, respectively. This is consistent with the XPS results (S/Mo(IV) = 2) of Li and Hercules (*21*).

Nitric oxide is often used to characterize sulfided molybdenum catalysts (*31, 32*). It has been revealed by XPS (*39*) that NO adsorbs on edge planes of MoS_2. However, Miciukiewicz *et al.* (*10*) demonstrated that the amount of NO adsorption depended on the adsorption temperature. In addition, from the productions of N_2O and N_2 on NO adsorption, it was shown that NO oxidized a partially reduced MoO_3/Al_2O_3 at room temperature and above (*40*). During the present TDS study of NO adsorbed on sulfided catalysts, the production of N_2O was observed as shown previously by Jung *et al.* (*5*). Thus, NO is not a perfect probe molecule for the characterization of molybdenum oxide and sulfide catalysts. Similarly, O_2 is an insufficient probe molecule. The NO/O_2 ratio has been reported to be four for a moderately reduced MoO_3/Al_2O_3 (*40*), suggesting a dissociative adsorption of O_2 at 195 K. This may result in the oxidation of the adsorption sites. Recently, CO has been proposed as a more reliable probe molecule (*41*).

Coupled with IR techniques, NO adsorption has been demonstrated to differentiate the chemical nature of the sites, e.g., oxidic vs sulfided sites (*31, 32*) and molybdenum vs cobalt (*42*) or nickel (*43*). Furthermore,

the adsorption amount of NO seems to be fairly successfully correlated to the HDS activities over promoted and unpromoted catalysts as mentioned above (*4, 5, 7–10, 42, 43*). Accordingly, NO was employed as a practical probe molecule in the present study. The amounts of NO adsorption in Table 2 should be regarded as relative values and would provide relative numbers of active sites. The amount of NO adsorption measured after the H_2-treatment at 673 K is expected to provide the maximum number of NO adsorption sites which may potentially act as active sites under the HDS reaction conditions (H_2-atmosphere) at 673 K.

The NO/Mo ratio is considered to depend on the extent of sulfidation of precursor oxide phases, slab size and dispersion of resultant molybdenum sulfide phases, and facility of sulfur vacancy formation. As shown in Fig. 5, the NO/Mo ratio of the MoO_3/TiO_2 catalyst decreased as the molybdenum content increased. This is explained in terms of the increase in the slab size of molybdenum sulfides with increasing molybdenum loading up to 40×10^{13} Mo cm^{-2}, since the I_{Mo}/I_{Ti} XPS ratio increased linearly in this concentration range. Taking into account the saturated I_{Mo}/I_{Ti} XPS ratio at a higher molybdenum content, a further increase in the MoS_2-slab size and a three-dimensional growth of MoS_2 crystals are considered to occur, resulting in a decrease of molybdenum dispersion. A similar interpretation is applicable to the MoO_3/Al_2O_3 catalysts containing $>12 \times 10^{13}$ Mo cm^{-2} (4.8 wt% MoO_3). A low NO/Mo ratio for the smallest molybdenum content catalyst is due to a low fraction of sulfided phase as expected from the Mo3*d* XPS in Fig. 2.

The NO/Mo ratio depended strongly on the support. The MoO_3/TiO_2 showed a significantly higher NO/Mo ratio than the MoO_3/Al_2O_3 at a low molybdenum content. On the basis of the XPS results, this is attributed to a higher extent of sulfidation of molybdenum oxide phase (Figs. 2 and 3) and to a higher extent of elimination of sulfur anions (ΔS/Mo) by the H_2-treatment at 673 K (Table 1) for the MoO_3/TiO_2 catalysts than for the MoO_3/Al_2O_3 catalysts, taking into consideration the comparable slab size of MoS_2. The higher ease of sulfur anion removal for MoO_3/TiO_2 compared to MoO_3/Al_2O_3 is ascribed to the differences in the structure of sulfided molybdenum and/or to interaction modes between sulfided molybdenum and support, which modify the Mo–S bond strength (vide infra).

The TDS of NO in Fig. 8 demonstrates the presence of at least two kinds of NO adsorption sites. The assignment of adsorption sites of α- and β-NO was conducted on the basis of the H_2S–NO coadsorption in Fig. 9. The desorption temperature of the α-peak was increased by ca. 30 K on the H_2S adsorption, while that of the β-NO peak was not influenced. Since the $\alpha/(\alpha + \beta)$ ratio was not affected by the H_2S-coadsorption, it is considered that H_2S causes no preferential desorption of α- or β-NO species. Taking into account the dependence of the $\alpha/(\alpha + \beta)$ ratio on the slab size of MoS_2 or on the edge atom/corner atom ratio, α- and β-peaks might be assigned to the adsorption on the edge planes and corners of MoS_2 slabs, respectively. However, it seems difficult to explain directly the effect of coadsorbed H_2S upon the desorption temperature of the α-peak alone. Accordingly, it is concluded that α- and β-peaks are assigned to the NO species adsorbed on coordinatively unsaturated (cus) Mo-sites with different numbers of unsaturation.

It has been well established by using ^{14}NO and ^{15}NO isotopes and IR techniques that two NO molecules adsorb on one Mo-site, forming dinitrosyl species (*33–35*). The adsorption sites for α- and β-NO species are proposed in Scheme 1. α- and β-sites are assigned to triply and doubly cus sites, respectively. Lower desorption temperature or lower thermal stability of α-NO may be ascribed to a remaining vacancy on the molybdenum sites. The H_2S molecule adsorbed on the vacant site is considered to stabilize the preadsorbed α-NO molecules.

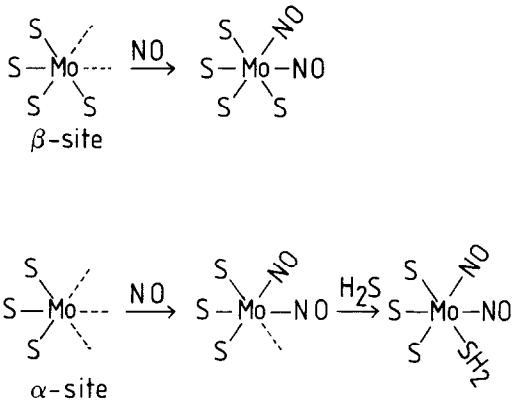

SCHEME 1. Proposed α- and β-sites on sulfided molybdenum catalysts.

As demonstrated by LRS in Fig. 1, MoS_2-like species are formed on the Al_2O_3- and TiO_2-supported catalysts. Both α- and β-NO adsorption sites are considered to be located at the edges or corners of MoS_2 slabs (*39*). Assuming a hexagonal structure for MoS_2 slabs, the edges consists of $(10\bar{1}0)$ and $(\bar{1}010)$ planes (Fig. 12). In the case of $(\bar{1}010)$ plane, the elimination of labile sulfur anions produces triply cus Mo-sites or α sites as well as doubly cus Mo-sites or β-sites, while exclusively β sites are formed on $(10\bar{1}0)$ edge planes. It is assumed here that only cus sulfur anions (S) are eliminated under the present conditions (H_2-treatment at 673 K) rather than coordinatively saturated bulk sulfur anions (S_b). It should be noted that the β-sites on the $(\bar{1}010)$ plane involve labile cus sulfur anions and convert into α-sites on a further elimination of the cus sulfur anion.

The $\alpha/(\alpha + \beta)$ ratio depends on both support and molybdenum loading, as shown in Table 2. The sulfided MoO_3/TiO_2 catalysts showed lower $\alpha/(\alpha + \beta)$ ratios than the MoO_3/Al_2O_3 catalysts. In both systems the ratio increased with increasing molybdenum content. These findings cannot be interpreted in terms of the NO/Mo ratio (relative slab size and dispersion of molybdenum sulfide). It is proposed here that the morphology of MoS_2-like species depends on the support and molybdenum loading. MoS_2 slabs produced on MoO_3/Al_2O_3 catalysts expose a higher proportion of $(\bar{1}010)$ edge plane than those on MoO_3/TiO_2 catalysts. With increasing molybdenum loading, $(\bar{1}010)$ edge plane becomes more important than $(10\bar{1}0)$ plane on both catalyst systems. At high molybdenum content ($>40 \times 10^{13}$ Mo cm^{-2}), XPS intensity analyses suggested the formation of three dimensional MoS_2 species. This implies that the morphology of multilayered MoS_2 is also affected by the support. The change in the

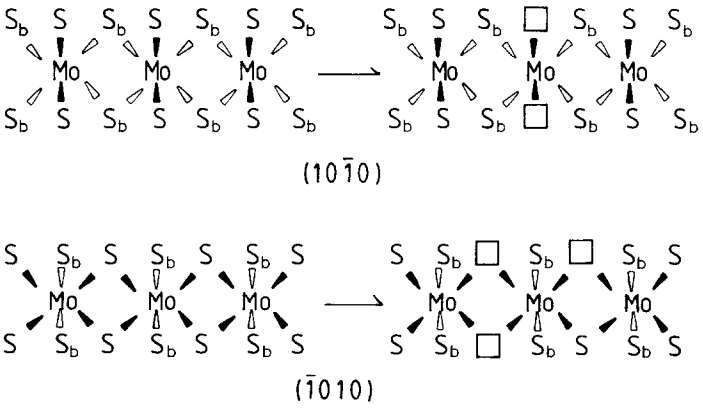

FIG. 12. Schematic drawings for $(10\bar{1}0)$ and $(\bar{1}010)$ edge planes and anion vacancies. S, coordinatively unsaturated sulfur anion, S_b, coordinatively saturated bulk sulfur anion, and □, anion vacancy.

morphology of the molybdenum sulfide may result from molybdenum oxide–support interactions and/or molybdenum sulfide–support interactions. The latter interactions are suggested to modify the facility of anion vacancy formation (Table 1).

Similar propositions have been made for supported sulfide catalysts. Comparing the HDS activity of nickel sulfide supported on SiO_2 and Al_2O_3, Burch and Collins (*44*) proposed that the morphology or composition of nickel sulfide was modified by metal sulfide–support interactions. Very recently, Bouwens *et al.* (*45*) demonstrated by using EXAFS and XANES that the structure of the cobalt sulfide phase supported on carbon was not a specific Co_9S_8 phase and that a higher percentage of octahedral cobalt species was present on cobalt sulfide/carbon system than on Co_9S_8. The structure specific to carbon-supported cobalt sulfides was related to significantly high HDS activities of these catalysts (*46*). Consequently, it is considered that the structure or morphology of metal sulfide generally depends on the support.

The configuration of active sites on the sulfided MoO_3/Al_2O_3 and MoO_3/TiO_2 catalysts is deduced for the hydrogenation of butadiene at 273 K on the basis of the results in Fig. 10. The direct correlation between the hydrogenation activity and the amount of α-NO, including both catalyst systems, suggests that the hydrogenation takes place preferentially on α-sites or triply cus Mo-sites. The configuration of the hydrogenation sites suggested here is consistent with that proposed by Tanaka and Okuhara (*47*). Recently, Wambeke *et al.* (*48*) have suggested that triply cus Mo-sites are responsible for the hydrogenation of isoprene over H_2-treated MoS_2/Al_2O_3 catalysts at 323 K, on the basis of both the dependence of the activity upon the S/Mo ratio and the structural model of MoS_2 (*38*). Accordingly, the excellent agreement concerning the active sites strongly suggests that triply cus Mo-sites constitute the active sites for the hydrogenation of olefins at relatively low temperatures (<323 K).

The extension of the proposal to hydrogenations under HDS conditions may require some discussions. As pointed out by Massoth and MuraliDhar (*49*), it is possible that hydrogenation sites at a high reaction temperature are different from those at a low temperature. It was reported that at a low temperature hydrogenations were poisoned by H_2S (*47*), while at a high temperature they were little affected (*49*). However, butadiene has been reported to be hydrogenated by H_2S at 673 K (*50*). In addition, it has been revealed by Barbour and Campbell (*51*) using isotopes that the H_2S molecule dissociatively adsorbs on cus Mo-sites of MoS_2 at 623 K in the following manner:

$$H_2S \rightleftharpoons H_{ads} + HS_{ads}. \qquad (1)$$

The following isotopic exchange reaction was also reported to proceed effectively over MoS_2 at 693–773 K (*52*):

$$H_2S + D_2 \rightleftharpoons D_2S + H_2. \qquad (2)$$

Taking into account these findings, the hydrogenation cycles over sulfided catalysts are proposed to occur as in Scheme 2, where only α-sites constitute olefin hydrogenation centers at low and high reaction temperatures and in the absence and presence of H_2S. It is assumed in Scheme 2 that labile cus sulfur atoms (S) work as hydrogen acceptors, while coordinatively saturated bulk sulfur atoms (S_b) are inactive. The catalytic cycle I involving α-sites is proposed by Tanaka *et al.* (*47*) and may operate at both low and high temperatures. In the presence of H_2S, α-sites are equilibrated with α-H_2S-sites which catalyze hydrogenations only at high temperatures, as proposed in cycle II. α-S-, namely, β-sites involving cus sulfur atoms are formed as an intermediate. The catalytic cycle II is ineffective at low temperatures, since the formation of α-H_2S-sites inhibits the hydrogenation because of a low hydrogen donating activity. On the other hand, it is considered that the β-sites formed on $(10\bar{1}0)$ cannot catalyze the hydrogenation at any temperature as a result of the coordinative satura-

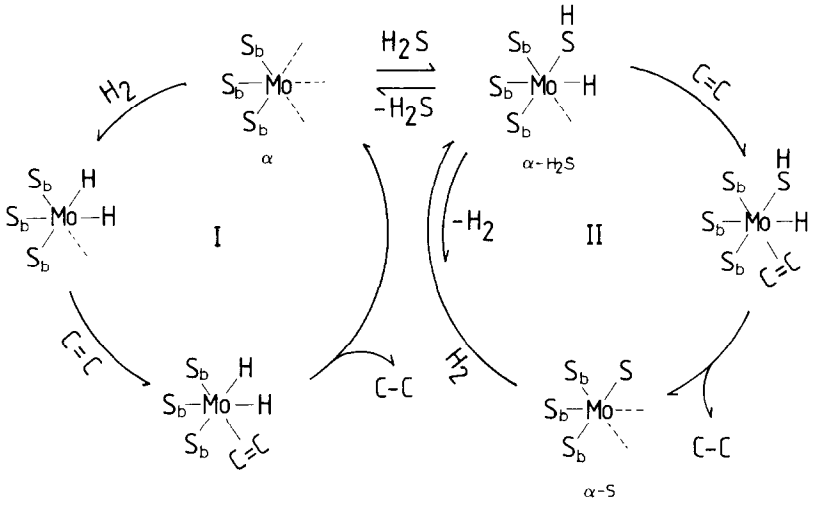

SCHEME 2. Plausible catalytic cycles I and II for the hydrogenation of olefins over sulfided molybdenum catalysts. S, coordinatively unsaturated sulfur anion, and S_b, coordinatively saturated bulk sulfur.

tion of sulfur atoms in the coordination sphere of the Mo-site.

The active sites for the HDS of thiophene on supported molybdenum sulfides are not as straightforward as those for the hydrogenation of butadiene at 273 K. No linear correlations could be obtained between the amount of total, α-, or β-NO and the activity as exemplified in Fig. 11. On the basis of the parabolic correlations, it is proposed here that the HDS of thiophene proceeds effectively on dual Mo-sites, for example, adjacent α–α-sites, α–β-sites, or β–β-sites rather than on single α- or β-sites. As expected from the curves in Fig. 11, improved linear correlations were obtained between the HDS activities and the square of the amount of NO adsorption. The dual site model may be substantiated by recent quantum chemical calculations by Zonnevylle *et al.* (*53*). They suggest that η^5-interaction modes of thiophene with a Mo-site, in which the thiophene ring is parallel to the surface, are advantageous in weakening the S–C bond. Furthermore, it has been suggested that a cooperation of adjacent Mo-sites is particularly favorable to the S–C bond weakening, where thiophene adsorbs and forms bridge bonds between two adjacent cus Mo-sites while making the η^5-interaction with one of them.

Another question about the HDS is the difference between the supports. As shown in Fig. 11, TiO_2-supported catalysts showed a higher HDS activity than Al_2O_3-supported catalysts. Since the HDS activity was not a single function of $\alpha/(\alpha + \beta)$, the difference in the TOF between TiO_2- and Al_2O_3-supported catalysts cannot be attributed solely to the difference in the edge plane orientations of MoS_2 slabs. It is, accordingly, considered that the interactions between sulfided molybdenum and support surface are responsible for the difference in the TOF as well as the crystalline morphology of MoS_2 slabs. It is suggested by Candia *et al.* (*54*) that with sulfided MoO_3/Al_2O_3 catalysts, the Mo atoms on the edge planes are bonded to the support surface through Mo–O linkages. Vissers *et al.* (*55*) adopted similar interactions of molybdenum sulfide with alumina surface to interpret the low HDS activities of Al_2O_3-supported catalysts compared to carbon-supported catalysts (*56*).

The reducibility and sulfidability of molybdenum species in oxidic precursors are considered to be a measure of the strength of molybdenum–support interactions via Mo–O–metal bonds, since these bonds are strongly suggested to be broken on reducing the sulfiding processes (*20, 37*). Taking into account higher reducibility of molybde-

num on TiO_2 than on Al_2O_3, it is considered that the molybdenum atoms on the MoS_2 edge planes have no strong interactions with the TiO_2 surface, whereas they do interact with the Al_2O_3 surface. The negative effect of the interactions on the HDS activity may be interpreted in terms of the modification of the electronic state of the Mo atoms located at the active center. As discussed by Pecoraro and Chianelli (*57*) and Vissers *et al.* (*55*), electronic modifications of the Mo atoms would induce the change in the Mo–S bond strength, which controls the adverse kinetic factors in the HDS reaction, that is, the anion vacancy formation and adsorption of reactant. Unfortunately, in the present XPS and the TDS and IR studies of NO adsorption, no evidence was obtained for the electronic effect of the support on the molybdenum sulfides. In the case of the hydrogenation of butadiene at low temperature, no support effect was detected and the activity was understood in terms of the number of triply cus Mo-sites, suggesting that the local structure of the active sites is a controlling factor in the low temperature hydrogenation.

CONCLUSIONS

Sulfided MoO_3/Al_2O_3 and MoO_3/TiO_2 catalysts were characterized by using various physicochemical techniques. It has been shown by LRS and XPS that the MoO_3/TiO_2 is fully sulfided to produce predominantly MoS_2-like phases, whereas the MoO_3/Al_2O_3 is partially sulfided to produce Mo(V) species as well as MoS_2-like phases. Nitric oxide was employed to characterize cus Mo-sites as a practical probe molecule. The NO/Mo ratio of sulfided MoO_3/TiO_2 was higher than that of MoO_3/Al_2O_3 at a similar molybdenum loading per surface area of the support. The TDS of NO demonstrated the presence of α- and β-NO adsorption sites on sulfided molybdenum catalysts. On the basis of the TDS of H_2S–NO coadsorption, α- and β-sites were assigned to triply and doubly cus Mo-sites, respectively. The $\alpha/(\alpha + \beta)$ ratio depended on the molybdenum content and support, suggesting that the morphology of MoS_2-like species were varied with the loading and support because of molybdenum oxide and/or sulfide–support interactions. On the basis of the linear correlation between the hydrogenation activity and the number of α-sites, triply cus Mo-sites are proposed to be the active sites for the hydrogenation of butadiene at 273 K. Catalytic cycles are proposed for the hydrogenation of olefins at low and high reaction temperatures and in the presence and absence of H_2S on the basis of the present and literature results. Parabolic correlations between the HDS activity and the amount of NO adsorption suggested a dual site model for the HDS of thiophene. The HDS activity of the TiO_2-supported catalysts was higher than that of the Al_2O_3-supported catalysts, suggesting the negative effects of molybdenum sulfide–support interactions on the HDS.

ACKNOWLEDGMENTS

We gratefully acknowledge Messrs. M. Kitamura and K. Nagata for carrying out a part of the experimental procedures. We also thank Mr. M. Oh-Hama in the Faculty of Science, Osaka University, for the measurements of laser Raman spectra.

REFERENCES

1. Massoth, F. E., *in* "Advances in Catalysis" (D. D. Eley, H. Pines, and P. B. Weisz, Eds.), Vol. 27, p. 265. Academic Press, New York, 1978.
2. Grange, P., *Catal. Rev. Sci. Eng.* **21,** 135 (1980).
3. Tauster, S. J., Pecoraro, T. A., and Chianelli, R. R., *J. Catal.* **63,** 515 (1980).
4. Bachelier, J., Duchet, J. C., and Cornet, D., *Bull. Soc. Chim. Belg.* **90,** 1301 (1980).
5. Jung, H. J., Schmitt, J. L., and Ando, H., *in* "Proceedings of Fourth International Conference on the Uses of Molybdenum" (H. F. Barry and P. C. H. Mitchell, Eds.), p. 246. Climax Molybdenum Comp., Ann Arbor, MI, 1982.
6. Zwierczak, W., MuraliDhar, G., and Massoth, F. E., *J. Catal.* **77,** 432 (1982).
7. Topsøe, H., Candia, R., Topsøe, N., and Clausen, B. S., *Bull. Soc. Chim. Belg.* **93,** 783 (1984).
8. Topsøe, N., and Topsøe, H., *J. Catal.* **75,** 354 (1982).
9. Saini, A. R., Johnson, B. G., and Massoth, F. E., *Appl. Catal.* **40,** 157 (1988).
10. Miciukiewicz, J., Zwierczak, W., and Massoth, F. E., *Bull. Soc. Chim. Belg.* **96,** 915 (1987).
11. Ng, K. Y. S., and Gulari, E., *J. Catal.* **95,** 33 (1985).

12. Nishijima, A., Shimada, H., Sato, T., Yoshimura, Y., and Hiraishi, J., *Polyhedron* **5,** 243 (1986).
13. Shimada, H., Sato, T., Yoshimura, Y., and Nishijima, A., *J. Catal.* **110,** 275 (1988).
14. MuraliDhar, G., Massoth, F. E., and Shabtai, J., *J. Catal.* **85,** 44 (1984).
15. Ng, K. Y. S., and Gulari, E., *J. Catal.* **92,** 340 (1985).
16. Liu, Y. C., Griffin, G. L., Chan, S. S., and Wachs, I. E., *J. Catal.* **94,** 108 (1985).
17. Bond, G. C., Flamerz, S., and van Wijk, L., *Catal. Today* **1,** 229 (1987).
18. Quincy, R. B., Houalla, M., and Hercules, D. M., *J. Catal.* **106,** 85 (1987).
19. Zingg, D. S., Makovsky, L. E., Tischer, R. E., Brown, F. R., and Hercules, D. M., *J. Phys. Chem.* **84,** 2898 (1980).
20. Okamoto, Y. and Imanaka, T., *J. Phys. Chem.* **92,** 7102 (1988).
21. Li, C. P. and Hercules, D. M., *J. Phys. Chem.* **88,** 456 (1984).
22. Okamoto, Y., Tomioka, H., Katoh, Y., Imanaka, T., and Teranishi, S., *J. Phys. Chem.* **84,** 1833 (1980).
23. Schrader, G. L. and Cheng, C. P., *J. Catal.* **80,** 369 (1983).
24. Maezawa, A., Kitamura, M., Okamoto, Y., and Imanaka, T., *Bull. Chem. Soc. Japan* **61,** 2295 (1988).
25. Clausen, B. S., Topsøe, H., Candia, R., Villadsen, J., Lengeler, B., Als-Nielsen, J., and Christensen, F., *J. Phys. Chem.* **85,** 3868 (1981).
26. Zwierczak, W., Qader, Q., and Massoth, F. E., *J. Catal.* **106,** 65 (1987).
27. Brown, F. R., Makovsky, L. E., and Rhee, K. H., *J. Catal.* **50,** 162 (1977).
28. Cheng, C. P., and Schrader, G. L., *J. Catal.* **60,** 276 (1979).
29. Brown, F. R., Makovsky, L. E., and Rhee, K. H., *J. Catal.* **50,** 385 (1977).
30. Okamoto, Y., Imanaka, T., and Teranishi, S., *J. Phys. Chem.* **85,** 3798 (1981).
31. Okamoto, Y., Katoh, Y., Mori, Y., Imanaka, T., and Teranishi, S., *J. Catal.* **70,** 445 (1981).
32. Valyon, J. and Hall, W. K., *J. Catal.* **84,** 216 (1983); Valyon, J., Schneider, R. L., and Hall, W. K., *J. Catal.* **85,** 277 (1984).
33. Millman, W. S. and Hall, W. K., *J. Phys. Chem.* **83,** 427 (1982).
34. Peri, J. B., *J. Phys. Chem.* **86,** 1615 (1982).
35. Kazusaka, A. and Howe, R. F., *J. Catal.* **63,** 447 (1980).
36. Okamoto, Y., Oh-Hara, M., Maezawa, A., Imanaka, T., and Teranishi, S., *J. Phys. Chem.* **90,** 2396 (1986).
37. Hall, W. K., *in* "Proceedings of the Climax Fourth International Conference of the Chemistry and Uses of Molybdenum" (H. F. Barry and P. C. H. Mitchell, Eds.), p. 224. Climax Molybdenum Comp., Ann Arbor, MI, 1982.
38. Kasztelan, S., Toulhoat, H., Grimblot, J., and Bonnelle, J. P., *Appl. Catal.* **13,** 127 (1984).
39. Suzuki, K., Soma, M., Onishi, T., and Tamaru, K., *J. Electron Spectrosc. Relat. Phenom.* **24,** 283 (1981).
40. Reddy, A., Goldwasser, J., and Hall, W. K., *J. Catal.* **113,** 82 (1988).
41. Zaki, M. I., Vielhaber, B., and Knözinger, H., *J. Phys. Chem.* **90,** 3176 (1986).
42. Candia, R., Clausen, B. S., Bartholdy, J., Topsøe, N. and Topsøe, H., *in* "Proceedings, 8th International Congress on Catalysis," p. 375. Verlag Chemie, Weinheim, Berlin, 1984; Topsøe, N., and Topsøe, H., *J. Catal.* **77,** 293 (1982).
43. Lopez Agudo, A., Gil Llambias, F. J., Tascon, J. M. D., and Fierro, J. L. G., *Bull. Soc. Chim. Belg.* **93,** 719 (1984).
44. Burch, R., and Collins, A., *J. Catal.* **97,** 385 (1986).
45. Bouwens, S. M. A. M., Koningsberger, D. C., de Beer, V. H. J., and Prins, R., *Catal. Lett.* **1,** 55 (1988).
46. Duchet, J. C., van Oers, E. M., de Beer, V. H. J., and Prins, R., *J. Catal.* **80,** 386 (1983).
47. Tanaka, K. and Okuhara, T., *Catal. Rev. Sci. Eng.* **15,** 249 (1977), and references therein.
48. Wambeke, A., Jalowiecki, L., Kasztelan, S., Grimblot, J. P., and Bonnelle, J. P., *J. Catal.* **109,** 320 (1988).
49. Massoth, F. E. and MuraliDhar, G., *in* "Proceedings of the Climax Fourth International Conference of the Chemistry and Uses of Molybdenum" (H. F. Barry and P. C. H. Mitchell, Eds.), p. 243. Climax Molybdenum Comp., Ann Arbor, MI, 1982.
50. Sugioka, M. and Kimura, F., *J. Japan Petrol. Inst.* **28,** 270 (1985).
51. Barbour, J., and Campbell, K. C., *J. Chem. Soc. Chem. Commun.,* 1371 (1982).
52. Katsumoto, M., Fueki, K., and Mukaibo, T., *Bull. Chem. Soc. Japan* **46,** 3641 (1973).
53. Zonnevylle, M. C., Hoffmann, R., and Harris, S., *Surf. Sci.* **199,** 320 (1988).
54. Candia, R., Sorensen, O., Villadsen, J., Topsøe, N., Clausen, B. S., and Topsøe, H., *Bull. Soc. Chim. Belg.* **93,** 763 (1984).
55. Vissers, J. P. R., Scheffer, B., de Beer, V. H. J., Moulijn, J. A., and Prins, R., *J. Catal.* **105,** 277 (1987).
56. Vissers, J. P. R., Bachelier, J., ten Doeschate, H. J. M., Duchet, J. C., de Beer, V. H. J., and Prins, R., *in* "Proceedings, 8th International Congress on Catalysis," p. 387. Verlag Chemie, Weinheim, Berlin, 1984.
57. Pecoraro, T. A., and Chianelli, R. R., *J. Catal.* **67,** 430 (1981).